

Effect of substrate on the properties of calcite thin films prepared by dip coating method

J. Kumari¹, P. Kumar^{1*}, R. Singhal², A. K. Mukhopadhyay³, M. G. H. Zaidi⁴¹Department of Physics, Manipal University Jaipur, Jaipur-303007, Rajasthan, India²Department of Physics, Malaviya National Institute of Technology, Jaipur-302017, India³Department of Physics, Sharda School of Basic Sciences and Research, Sharda University, Greater Noida 201310, Uttar Pradesh, India⁴Department of Chemistry, College of Basic Science and Humanities, G.B Pant University of Agriculture and Technology, Uttarakhand, 263145, India

Received: March 12, 2023; Revised: March 31, 2023

We report on the development of calcite thin film on two different glass substrates. The first film was deposited on pre-cleaned glass substrate and another film was deposited on the glass substrate treated with dilute hydrofluoric acid (HF), using dip-coating. The films were synthesized by dipping glass substrate and etched glass substrate alternatively into calcium metal salt solution $\text{Ca}(\text{NO}_3)_2 \cdot 4\text{H}_2\text{O}$ and NaOH base solution. Several techniques were used to characterize the thin films that include X-ray diffraction, Fourier transform infrared spectroscopy (FTIR), field emission scanning electron microscopy (FESEM) and ultraviolet-visible spectroscopy (UV-Vis). From FESEM images of substrates it was observed that the etched sample has higher roughness than the plain glass substrate. Accordingly, the effect of roughness was monitored on the morphology of deposited calcite thin films. The rough surface of substrate lead to a bigger crystallite size of calcite thin films as calculated by XRD peaks and also observed in FESEM image. Subsequently, from optical studies, the bandgap of the thin films was found to decrease with increase in crystallite size. The present study on the calcite thin films might pave the way to understand the thin films and further use them in several applications in sensors, biomedical, environmental, and for fundamental research.

Keywords: Calcite, thin films, dip method, substrate effect, XRD

INTRODUCTION

Calcium carbonate (CaCO_3) is one of the substances that are found in plenty amount on the earth. Minerals that contain this element are found in rocks and are important components of pearls and shells of marine organisms. In general, calcium carbonate forms three distinct crystal forms, aragonite, vaterite, and calcite. Each crystal form has a characteristic morphology, such as rhombohedral, spherical, or needle-like [1]. Several industries use this mineral. It is a primary component in agricultural lime [2], utilized as a filler material in paper and collar industries, and extensively used as a building substance in the production industry [3, 4]. There are several important factors to consider, one of which is particle morphology, and recent studies have been directed toward crystal shape [5]. Many approaches have been developed to synthesize the calcite, including biomimetic synthesis [6], carbonization [7], and precipitation [8], reverse micro emulsion [9], microwave irradiation [10]. Ultrasonic intensity can also be used on it or surface morphology of calcium carbonate. A report by Tolba *et al.* and Mantilaka *et al.* has shown that it is common to find calcite CaCO_3 in cubic and flaky forms [13, 14]. As far as we know, there has been

little research on calcite CaCO_3 thin films. Hence, gap of knowledge about calcite in literature becomes the scope of the present research.

In this study, we synthesized the thin films of calcium carbonate using chemical dip-coating method. The prepared thin films were characterized using several characterization techniques. The effect of substrate on the deposition of calcite thin films was studied.

EXPERIMENTAL

Preparation of substrate

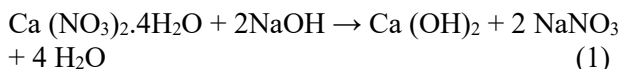
The calcite thin films were deposited on fresh glass substrate and etched glass substrate. Etched glass substrate was prepared by keeping the fresh glass substrate in a solution of HF (48%) and D.I. water in the ratio of (10:30) for 10 min. Before deposition, the substrates were thoroughly cleaned with deionised water and dried at room temperature. [15, 16].

Formation of CaCO_3 thin films

For the preparation of CaCO_3 thin films, the precursors of analytical grade reagents were used without any additional purification. The precursors 0.2M calcium nitrate tetrahydrate $\text{Ca}(\text{NO}_3)_2 \cdot 4\text{H}_2\text{O}$ and 0.2 M sodium hydroxide (NaOH) were weighed

* To whom all correspondence should be sent:
E-mail: pushpendra.kumar@jaipur.manipal.edu

accurately and dispersed in D.I. water while the solution was constantly stirred. Two glass substrates were used to deposit thin films. The first one was fresh glass substrate and the second one was etched glass substrate. The fresh glass substrate was fixed in the sample holder and the dipping rate of the substrate in the individual solution was kept at 400 mm/min for 20 dips, alternatively in sodium hydroxide (NaOH) and calcium nitrate tetrahydrate $\text{Ca}(\text{NO}_3)_2 \cdot 4\text{H}_2\text{O}$ solution and sample name was assigned as G1. The etched glass substrate was also fixed in a sample holder, dipped for 20 times alternatively in NaOH and $\text{Ca}(\text{NO}_3)_2 \cdot 4\text{H}_2\text{O}$ aqueous solutions and the resulted calcite deposited thin film was named as sample G2. During this process calcium hydroxide thin film is formed, however it immediately reacted with CO_2 gas present in the environment and converted to calcium carbonate thin films. The following reactions take place during the calcite thin film formation.



Characterization of CaCO_3 thin films

Rigaku Minifilm-II X-ray diffractometer with $\text{Cu K}\alpha$ radiation of wavelength 1.54054 \AA was used to analyse the structural properties, crystallite size and phase of the synthesized thin films. Optical studies were done by a Shimadzu UV-NIR 2600 spectrophotometer. Using a JEOL (JSM-7610FPlus) FESEM, we examined the thin films microstructure of surface morphologies. FTIR was utilized to analyse the functional groups present in calcite thin films using a Bruker Alpha instrument (resolution of 0.8 cm^{-1} in the wavenumber range $4000\text{-}500 \text{ cm}^{-1}$).

RESULTS AND DISCUSSION

Structural study

In Figure 1, the XRD spectra of all the prepared samples are shown. According to the XRD spectra, different peaks can be classified into the following planes: (012), (104), and (108) at 2θ values of 22.35° , 29° and 48.45° , respectively. The main peak (108), which was observed at $2\theta \sim 29^\circ$, is of the rhombohedral calcite phase of CaCO_3 (space group R-3C and no.: 167, PDF Card No. 00-005), and precisely matches the diffraction peak reported in literature [17, 18]. As indicated in Figure 1, XRD was used to determine the pure phase of the calcite thin film in both samples and to confirm that the synthesized thin films are nanocrystalline in nature. Average crystallite size (t_{ds}) of the samples was evaluated according to Scherrer equation [19]:

$$t_{ds} = \frac{k\lambda}{\beta \cos\theta} \quad (3)$$

Here, k is a correction factor that is often considered to be 0.9, and λ , β , θ represent the x-ray wavelength, full width at half maximum, and diffraction angle in turn. The calculated crystallite size of the thin film samples G1 and G2 was found to be 7.12 nm and 7.52 nm, respectively.

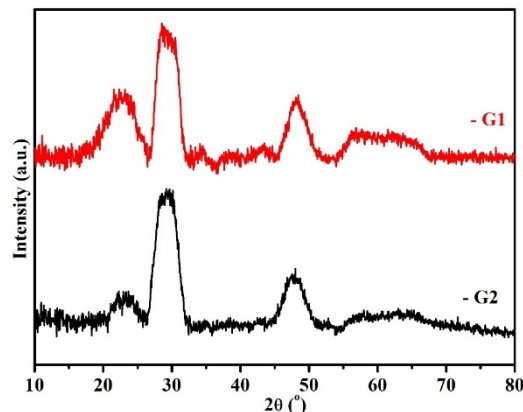


Fig. 1. XRD spectra of calcite thin films (G1) on plain glass and (G2) on etched glass substrate.

Morphological studies:

Fig. 2 (a) presents an FESEM image of the calcite thin film of sample G1 and Fig. 2(d) presents a FESEM image of the calcite thin films of sample G2 which is deposited on etched glass substrate. An illustration of the nanocrystalline structures with cubic shapes can be seen in Figure 2(a). As can be seen from Figures 2(a) and 2(d), both samples have uniform morphology. However, there is a small difference in the surface roughness. The sample G2 shows a higher surface roughness than the sample G1. Analogous results were also reported in the literature by Abdallah *et al.* in a ZnO thin film system on a different substrate [20]. Fig. 2(b) exhibits a higher magnification of Fig. 2(a) for a better representation of a cubic structure. In Fig. 2 (c), the EDAX pattern of sample G1 is shown and the substantial occurrence of C along with Ca and O is seen. Calcite thin film formation was further confirmed by the peak of carbon in EDAX pattern in the current paper and well supported by XRD data discussed in prior section. Similarly, in Fig. 2 (d) we exhibit the FESEM image demonstrating the spherical microstructure of sample G2. Fig. 2(e) displays the higher magnification of Fig. 2(d) for a better representation. As can be seen from the FESEM image, Fig. 2(d) shows higher roughness than Fig. 2(a). This difference in roughness can be attributed to the surface morphology of the substrate. Similarly, in Fig. 2(f) we exhibit the respective EDAX pattern of sample G2. It is further confirmed by the presence of carbon along with Ca and O in the

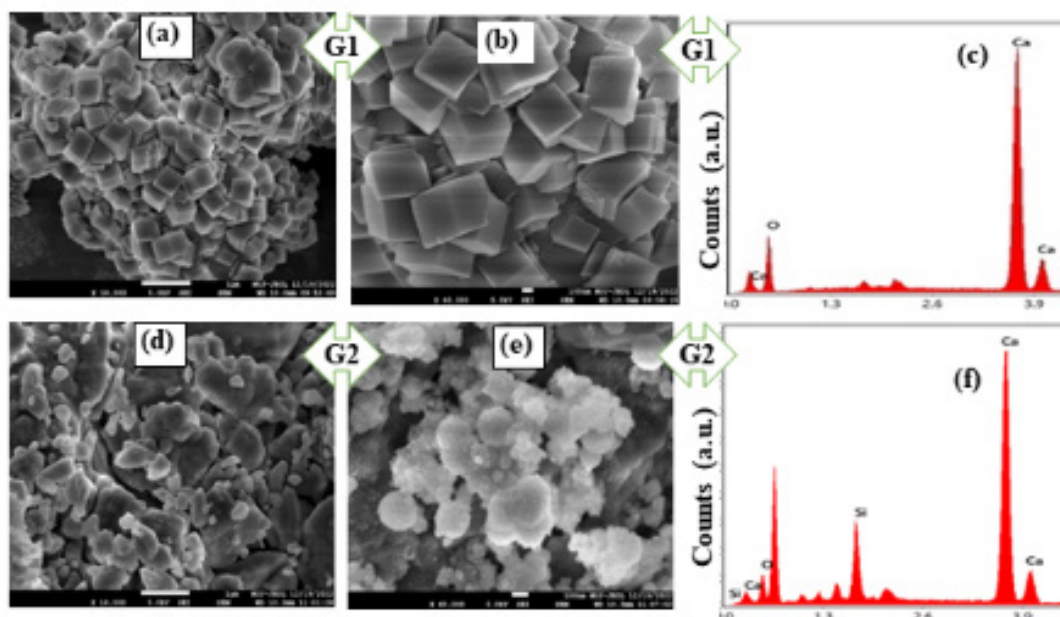


Fig. 2. FESEM and EDAX patterns of G1 and G2.

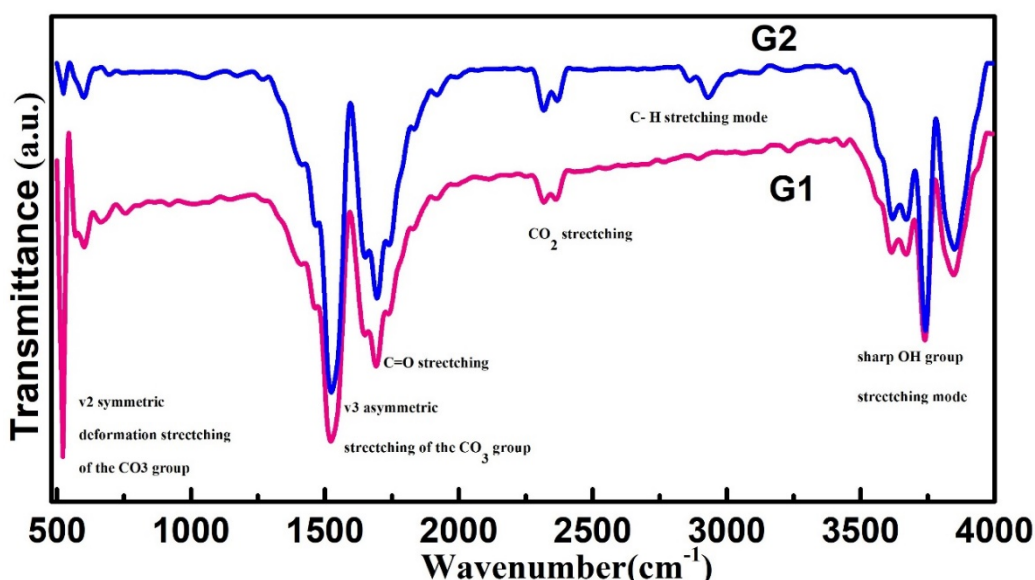


Fig. 3. FTIR spectra of calcite thin films of G1 and G2.

EDAX pattern that calcite phase formation took place in the prepared thin film, which is also in agreement with the XRD results. Hence, EDAX and XRD results in both samples correlated well with each other and revealed a calcite phase with controllable microstructure of calcite thin films. Spherical-like microstructure appears rougher in sample G2 as can be seen in Fig. 2(d).

FTIR studies

Figure 3. illustrates the FTIR spectra of G1 and G2 samples. Both the spectra show an absorption band at 550 cm^{-1} corresponding to the CO_3 group stretching mode. The CO_3 absorption v_3 symmetric

stretching on the thin film sample causes the broad peak at 1500 cm^{-1} . The peak in the CO stretching mode appears at 1750 cm^{-1} . During atmospheric adsorption of CO_2 , a small peak at 2400 cm^{-1} is observed. In the surface OH group stretching mode, there is a sharp absorption band at 3750 cm^{-1} . Every functional group available in both thin film samples G1 and G2. However, here is a minor difference in the peak's intensity of both samples. This can be due to samples deposited on different substrates.

The similar functional group for calcite is reported in literature [21]. The CO₃ absorption ν₂ symmetric stretching peak is decreasing with the change in substrate surface that can be seen in Figure 3. The FTIR spectra of each sample showed the functional group of Ca(OH)₂ and CaCO₃, as indicated.

Optical studies

Figure 4 shows the UV-Vis absorption spectra for synthesised CaCO₃ thin films on both the substrates in the wavelength range of (190-800 nm). A small increase in optical absorbance was observed in sample G2 with respect to G1, as illustrated in Figure 4. The latter shows the average absorption range dependency on surface roughness of the deposited thin film. In Figure 5 we show the related Tauc's plot of both samples. A red shift in the absorbance band edge was observed in sample G2, as seen in Fig. 4. This red shift in the band edge of absorbance was due to an increase in the crystallite size in sample G2. The following equation may be used to calculate the optical band gap of both samples:

$$(\alpha h\nu) = A (h\nu - E_g)^n \quad (4)$$

Here n is a constant associated to the type of transition (n=1/2 for a direct band gap), α is the optical absorption coefficient, 'A' represents a constant and E_g is the energy gap. In order to calculate band gap energy, the straight section of the curve between "hν" and (αhν)² was extrapolated. As shown in Figure 5, the band gap energies of the CaCO₃ thin films are 3.74 eV and 3.72 eV for the sample G1 and G2, respectively. The similar observation of band gap as a function of crystallite size was also published in literature by other workers [22-24]. According to the XRD examination, the crystallite size in sample G2 was found to be greater than that in sample G1. Hence, bandgap values are changed accordingly. These changes in band gap are also supported by FESEM results, where the surface roughness gets bigger as the crystallite size increases

due to rough surface and accordingly the bandgap decreases.

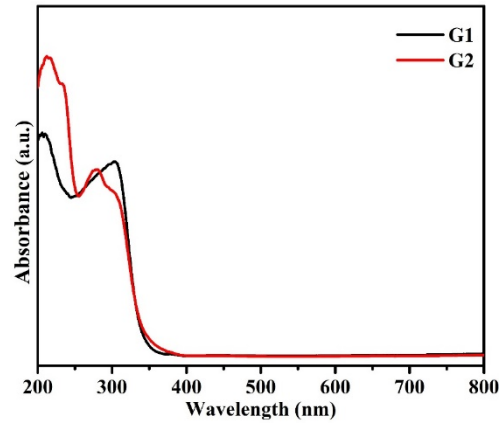


Fig. 4. Absorption spectra of calcite thin films of G1 and G2.

CONCLUSIONS

The calcite thin films were synthesized successfully using simple dip coating. Two different substrates were used in the present study. One is fresh glass substrate and the second is etched glass substrate. In etched glass substrate, the calcite thin film was found to be rougher than the plain glass substrate. From the FESEM images, it was seen that by changing the substrate surface different types of surface morphology of deposited thin films can be obtained. Small differences in the functional group intensity were observed that were attributed to the substrate surface effect. Further, it was seen from XRD results that the crystallite size in the film deposited on etched surface was larger than the thin film deposited on fresh glass substrate. Accordingly, the band gap of calcite thin film was found to decrease from 3.74 eV to 3.72 eV with increase in crystallite size. Moreover, the results suggest that calcite thin films can be tailored for future biomedical applications in both band gap and microstructure.

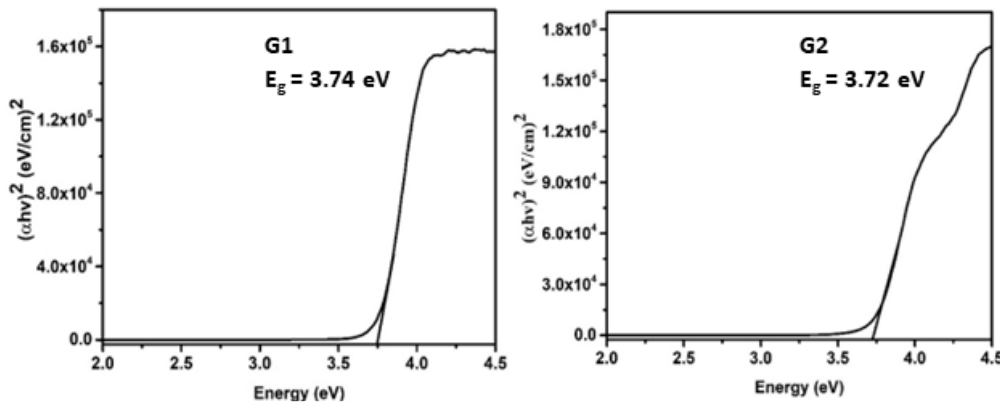


Fig. 5. Tauc's plot of (αhν)² vs. (hν) energy for CaCO₃ thin films of G1 and G2.

Acknowledgement: The corresponding author (Pushpendra Kumar) acknowledges the funding support from DST SERB with reference no. SUR/2022/004227 sanctioned on October 6, 2023, and to the sophisticated analytical instrument facility (SAIF) and Central Analytical Facility at Manipal University Jaipur for extending the necessary analytical facilities. The first author Jyoti, thanks the Manipal University Jaipur for funding support through the Dr Ramdas Pai scholarship.

REFERENCES

1. L. Minkowicz, A. Dagan, V. Uvarov, O. Benny, *Materials (Basel)*, **14**, 3525 (2021).
2. K.Y. Chan., D.P. Heenan, *Aust. J. Soil Res.*, **36**, 73 (1998).
3. H. C. Sang, K. P. Jin, K. L. Seung, M. J. Sung, H. K. Im, W. A. Ji, K. Hwan, *Mater. Sci. Forum*, **10**, 881 (2007).
4. T. Matschei, B. Lothenbach, F. P. Glasser, *Cem. Concr. Res.*, **37**, 551 (2007).
5. J. S. Christopher, F. L. Sophie, C. M. Fiona, et al., *Adv. Funct. Mater.*, **20**, 2108, (2010).
6. Q Shen, L. C. Wang, X. P, Li, et al., *Cryst. Growth & Design*, **8**, 3879 (2008).
7. R. Y. U. Miyoung , J. H. Ahn, K. S. You, et al., *J. Ceram. Soc. Japan*, **117**, 106 (2009).
8. Yunlan Su, HR Yang, WX Shi, et al., *Colloids and Surfaces A: Physicochem. Eng. Aspects*, **355**, 158, (2010).
9. Y. T. Clifford, C. K. Chen, *Chemical Engineering Science*, **63**, 3632 (2008).
10. A. Rizzuti, C. Leonelli, *Powder Technology*, **186**, 255 (2008).
11. K Yoshiyuki, Y Kohei, N. Nobuyuki, *Ultrasonics Sonochemistry*, **17**, 617 (2010).
12. S. X. Li, Lyu, F Geng, et al., *J. Cryst. Growth.*, **312**, 1766, (2010).
13. E. Tolba, W.E.G. Muller, B.M.A. ElHady, M. Neufurth, F. Wurm, S. Wang, H. C Schröder, *Mater. Chem. B Mater. Biol. Med.*, **4**, 376 (2016).
14. M.M.M.G.P.G. Mantilaka, H.M.T.G.A. Pitawala, R.M.G. Rajapakse, D.G.G.P. Karunaratne, K.G.U. Wijayantha, *Cryst. Growth*, **392**, 52, (2014).
15. Hai Yan Xu, Si Le Xu, Xu Dong Li, Hao Wang, Hui Yan, *Science*, **252**, 4091 (2006).
16. Dong Bo Fan, Hao Wang, Yong Cai Zhang, Jie Cheng, Bo Wang, Hui, *Materials Chemistry and Physics*, **80**, 44 (2003).
17. J. Kumari, Harish, Akash, A. Pandey, P. Kumar, M. K Singh, A. Singh, M. S. Shishodia, R. P. Joshi, A. K. Mukhopadhyay, *Material Science Chemistry Select.*, **7**, 24, (2022).
18. J. Kumari, Harish, Akash, A. Pandey, P. Kumar, M. K. Singh, R. P. Joshi, A. K. Mukhopadhyay, *Material Today Proceeding*, **60**, 6 (2022).
19. Akash, Harish, J. Kumari, A. K. Mukhopadhyay, P. Kumar, *Chemistry Select.*, **7**, e202200417 (2022).
20. B. Abdallah, A. Kader, J. Feras, *J. Nanostuct.*, **10**, 185 (2020).
21. A. Barhoum, H. Rahier, R. E. Abou-Zaied, Mohamed R. Thierry Dufour, G. Hill, A. Dufresne, *ACS Appl. Mater. Interfaces*, **26**, 2734, (2014).
22. Harish, P. Kumar, J. Kumari, P. Phalswal, P. K. Khanna, A. Salim, R. Singhal, A. K. Mukhopadhyay, R. P. Joshi, *J. Nano-Electron. Phys.*, **13**, 01029, (2021).
23. P. Kumar, *ISRN Nanotechnology*, 2011 (2011) Article ID 163168, 6 pages.
24. P. Kumar, P. Lemmens, *RSC Advance*, **5**, 91134 (2015).